These results indicate that the SiC agostic interaction takes place regardless of the polarization function.

Concluding Remarks

We have optimized the structures of $Ti(C(SiH_2CH_3){=}CH_2)(Cl)_2^+$, model of $Ti(C(Si(CH_3)_3){=}C(CH_3))(C_6H_5)(Cp)_2^+$, to find the distorted alkenyl group that is the sign of the $SiC^{\gamma}\cdots Ti$ interaction. An analysis of geometries and molecular orbitals shows that the donative interaction from the SiC^{γ} σ bond to a Ti vacant d orbital is the major origin of alkenyl distortion, assisted by the CH $\rightarrow$ Ti d agostic interaction. The intramolecular $SiC^{\gamma}\cdots Ti$ interaction is similar in nature to the intramolecular $CH\cdots M$ interaction, called the agostic interaction. Therefore, the interaction found in the present study may be called the βSiC agostic interaction.

A similar distorted ligand, $CH[Si(CH_3)_3]_2$, in the neodymium complex, $NdCH[Si(CH_3)_3]_2Cp''_2Si(CH_3)_2$, **16** has been reported experimentally: a small NdCSi angle of 98° and a short $Nd\cdots C^{\gamma}$ distance of 2.90 Å.[15] The $Al_2(CH_3)_6$-like interaction between C and Nd has been suggested, as follow.

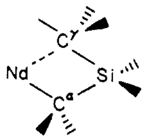

16

The structure of the $C^{\alpha}SiC^{\gamma}$ moiety in **16** resembles that of the alkenyl group in **5**. Since **16** is an electron-deficient complex, interactions similar to those we presented here are probably taking place in this lanthanide complex between the CSi σ bond and the Nd atom.

We also found the βCC agostic interaction in the optimized structure of $Ti(C(CH_2CH_3){=}CH_2)(Cl)_2^+$ and the βSiH agostic interaction in the optimized structure of $Ti(C(SiH_3){=}CH_2)(Cl)_2^+$. The βSiC agostic interaction is stronger than βCC agostic interaction, because the electron-donating ability of the SiC bond is stronger than the CC bond. It appears that the agostic interaction can take place between various σ bonds and vacant orbitals of an electron-deficient metal atom within a molecule. The extent of the structural distortion and stabilization, in competition with other conformational and structural energetics, would depend critically on the electron-donating ability of the σ bond and the electron-accepting ability of the metal as well as the ligands and the coordination unsaturation. Since these generalized agostic interactions are not known experimentally, they remain a prediction.

Acknowledgment. We acknowledge Prof. J. J. Eisch for comments on the present work. All the numerical calculations were carried out at the Computer Center of IMS.

Registry No. **1**, 99248-82-5; **5**, 111524-71-1; **12**, 111524-72-2; **13**, 111524-73-3; **16**, 98690-06-3; $Ti(C(SiH_2CH_3){=}CH_2)(Cp)_2^+$, 111524-74-4.

---

[15] Jeske, G.; Schock, L. E.; Swepston, P. N.; Schumann, H.; Marks, T. J. *J. Am. Chem. Soc.* **1985**, *107*, 8103.

Environmental Control of Product States in the Chemiluminescent Electron Transfer between Rubrene Radical Ions

Joon Kim and Larry R. Faulkner*

Contribution from the Department of Chemistry, University of Illinois, Urbana, Illinois 61801.

Received June 8, 1987

Abstract: Electrogenerated chemiluminescence (ecl) from the annihilation of rubrene anion and cation radicals has been studied in *N,N*-dimethylformamide solutions from −50 °C to room temperature. The magnetic enhancement of chemiluminescence declined toward lower temperatures. This result, together with the time dependence of ecl in triple-step experiments, suggests that ecl arises by both the S and T routes and that the T-route fraction declines at lower temperatures. Comparisons with the magnetic effect on ecl from a related system (the annihilation of the rubrene anion radical with the cation radical of *N,N,N′,N′*-tetramethyl-*p*-phenylenediamine) suggest that the T-route contribution to ecl in the rubrene system falls to about 10% near −40 °C. A new method for evaluating the relative ecl efficiency was developed. It showed that the efficiency generally rises in the rubrene system as the temperature is lowered, a result indicating that the change in the mechanistic balance is rooted in temperature-dependent branching ratios for production of singlet and triplet excited states in electron transfer. The efficiency of excited singlet production apparently doubles as the temperature drops over the working range. The concentration of supporting electrolyte also markedly influences the branching ratios for electron transfer.

The electrogenerated chemiluminescence (ecl) of rubrene has fascinated investigators for 2 decades, because it offers delicate energy balances in the two main steps of the chemiluminescence mechanism.[1,2] At least two distinct pathways to the emitting rubrene singlet ($^1R^*$) seem to exist, and their relative contributions are affected by the reaction environment. The system offers a rare opportunity to examine the manner in which extremely

---

[1] The most complete and the most recent reviews of ecl are the following: (a) Faulkner, L. R. *MTP Int. Rev. Sci., Phys. Chem., Ser. Two* **1975**, *9*, 213. (b) Faulkner, L. R.; Bard, A. J. *Electroanal. Chem.* **1977**, *10*, 1. (c) Pragst, F. *Z. Chem.* **1978**, *18*, 41. (d) Faulkner, L. R. *Methods Enzymol.* **1978**, *57*, 494. (e) Park, S. M.; Tryk, D. A. *Rev. Chem. Intermed.* **1981**, *4*, 43. (f) Faulkner, L. R.; Glass, R. S. In *Chemical and Biological Generation of Excited States*; Adam, W., Cilento, G., Eds.; Academic Press: New York, 1982; Chapter 6. (g) Tachikawa, H.; Faulkner, L. R. In *Laboratory Techniques in Electroanalytical Chemistry*; Kissinger, P. T., Heineman, W. R., Eds.; Marcel Dekker: New York, 1984; Chapter 23.

[2] The following papers concern the rubrene system in particular: (a) Hercules, D. M. *Science* **1964**, *145*, 808. (b) Visco, R. E.; Chandross, E. A. *J. Am. Chem. Soc.* **1964**, *86*, 5350. (c) Hercules, D. M.; Lansbury, R. C.; Roe, D. K. *Ibid.* **1966**, *88*, 4578. (d) Visco, R. E.; Chandross, E. A. *Electrochim. Acta* **1968**, *13*, 1187. (e) Chang, J.; Hercules, D. M.; Roe, D. K. *Ibid.* **1968**, *13*, 1197. (f) Bezman, R.; Faulkner, L. R. *J. Am. Chem. Soc.* **1972**, *94*, 6324; **1973**, *95*, 3083. (g) Faulkner, L. R.; Tachikawa, H.; Bard, A. J. *Ibid.* **1972**, *94*, 691. (h) Tachikawa, H.; Bard, A. J. *Chem. Phys. Lett.* **1974**, *26*, 246. (i) Periasamy, N.; Shah, S. J.; Santhanam, K. S. V. *J. Chem. Phys.* **1973**, *58*, 821. (j) Periasamy, N.; Santhanam, K. S. V. *Proc. Indian Acad. Sci., Sect. A* **1974**, *80*, 194. (k) Glass, R. S.; Faulkner, L. R. *J. Phys. Chem.* **1982**, *86*, 1652.

0002-7863/88/1510-0112$01.50/0

exothermic solution-phase reactions distribute products via multiple channels.[1f] In this paper, we will provide evidence that one can manipulate the primary electron-transfer reaction to provide different distributions of products by changing the details of the reaction environment. The observations reported here are pertinent, not only to ecl, but also to other areas in which very energetic electron-transfer reactions are of interest, such as natural and artificial photosynthesis.

The primary event is the annihilation of the cation and anion radicals of rubrene,[1,2] which is sufficiently energetic to yield products in several electronic states. At least the following reaction channels are accessible:

$$R\cdot^{+} + R\cdot^{-} \longrightarrow \left\{\begin{array}{ll} {}^1R^* + R & (1) \\ {}^3R^* + R & (2) \\ R + R & (3) \end{array}\right.$$

where $^1R^*$ and $^3R^*$ are the first excited singlet and the lowest triplet states. The chemiluminescence has the same spectrum as fluorescence; thus $^1R^*$ is the emitter,

$$^1R^* \rightarrow R + h\nu \qquad (4)$$

The simplest general mechanistic pathway for ecl is the "S route", which is direct generation and luminescence of the emitting state,[1] as expressed in reactions 1 and 4.

In some cases, ecl is seen even when the electron-transfer step is insufficiently energetic to yield the emitting singlet state directly. Much evidence[1] points to the operation of a second general mechanistic pathway, the "T route", in which the electron transfer produces a triplet (reaction 2), from which the emitting singlet is generated via triplet–triplet annihilation (TTA). Since TTA is always an energetic process, it also features several product channels. At least the following are possible in the rubrene system:[3]

$$^3R^* + {}^3R^* \longrightarrow \left\{\begin{array}{ll} {}^1R^* + R & (5) \\ {}^3R^* + R & (6) \\ R + R & (7) \end{array}\right.$$

Because the rubrene ion annihilation is capable of producing both singlet and triplet excited states, the S route and the T route could both contribute significantly to the ecl. We will provide evidence here that they do. Magnetic field effects have been used diagnostically to detect processes related to TTA in ecl mechanisms,[1,2g-j] and they will play an important part in this paper.

Since the energy released from the rubrene ion annihilation is close to the energy of the rubrene singlet (2.30 eV),[1,2] the S route is only marginally accessible. The energy of the lowest rubrene triplet is not known precisely, but it is estimated to be almost exactly half that of the first excited singlet;[3] therefore, TTA can produce $^1R^*$, but just barely. The energy relationships of this system are intriguing, because both the ion annihilation and TTA are so delicately balanced with respect to the channels generating the emitting singlet. Thus the distributions of events producing singlet, triplet, and ground states may be sensitive even to slight changes in the energetics of these steps. Perhaps it is not surprising that conflicting reports have arisen about mechanisms in the system.[1,2]

On the basis of magnetic field effects, a number of workers have suggested that the T route operates in this system.[2g-j] The intensity enhancements were typically 2–12% in the presence of a 0.1–0.7 T (1–7 kG) external magnetic field. Tachikawa and Bard found that the extent of the enhancement decreased with solvent polarity.[2h] They interpreted these results in terms of parallel S and T routes. They further suggested that the branching ratio for production of excited singlets in electron transfer (reaction 1) increases as polarity decreases. A plausible basis was a systematic rise in the electron-transfer free energy, due to poorer solvation of radical ions, as solvent polarity fell.

In the most recent work, Glass[2k] found that the rubrene system in DMF adhered very closely to S-route kinetics at low temperature, but displayed departures as room temperature was approached. The behavior was consistent with a T-route contribution, so Glass suggested that the S and T routes both operate for rubrene in DMF and that there is a temperature dependence to their relative contributions. The origin of the temperature dependence could not be pinpointed, but several possibilities were suggested, including temperature-dependent branching efficiencies in electron transfer or TTA.

We undertook the work described here in the hope of explaining the apparent temperature-related transition in the mechanism of the system. We have studied the magnetic field effect and the ecl efficiency as a function of temperature. The magnetic effects were examined on ecl from both the rubrene ion annihilation and the "mixed" system in which the rubrene anion radical is oxidized by the cation radical of *N*,*N*,*N'*,*N'*-tetramethyl-*p*-phenylenediamine (TMPD). Our evidence confirms the view that the rubrene system yields ecl almost exclusively via the S route at low temperature and that the T route becomes significant as room temperature is approached. The mechanistic variation seems to rest on temperature-dependent branching ratios in the primary electron-transfer process. Finally, we show results that indicate a surprisingly important effect of added electrolytes on that electron transfer.

Experimental Section

Chemicals. The rubrene (5,6,11,12-tetraphenylnaphthacene) and the TMPD were both supplied by Aldrich and purified by fractional sublimation in vacuo. The purified chemicals were stored in a vacuum desiccator over $CaSO_4$ and were dried again in vacuo for 24 h before each set of experiments.

N,*N*-Dimethylformamide (DMF), also from Aldrich, was used as the solvent after purification as described elsewhere.[4,5] Purified DMF was stored in a flask filled with argon and sealed with a serum cap made of silicone rubber. DMF was transferred to the evacuated sample cell, also capped with a serum cap, through a steel needle under positive argon pressure.[4]

Tetra-*n*-butylammonium tetrafluoroborate ($TBABF_4$) was used as the supporting electrolyte. It was synthesized according to the method of House[6] and recrystallized by dropping Millipore water into an ethanol solution of the salt.

Electrode Treatment and Sample Preparation. The voltammetric cell was designed to fit into the cell holder described below. It resembled that of Bezman,[5a] and the details of its design are available elsewhere.[4]

The area of the platinum disk working electrode was either 3.0 or 4.2 mm^2. The electrode was polished first with 6-μm, then 1-μm diamond paste, both supplied by Buehler. The final step was to press the electrode into a dry bed of 0.05-μm alumina spread on filter paper, and to give it a twist of one revolution. The alumina particles on the electrode were washed off with absolute EtOH and dried in a N_2 stream. Once prepared, the electrode was not polished again with diamond paste, but the final step, involving alumina, was employed before each experiment. The basis for this method has been discussed.[7]

After the polished electrode was assembled into the cell body, the cell was evacuated to high vacuum overnight. The weighed dry chemicals were added on the day of the experiment, and the cell was reevacuated. The solution was prepared by transferring DMF as described above. After at least five freeze–pump–thaw cycles, the cell was sealed under vacuum with a Teflon needle valve. Ordinarily the solution was used immediately, but if the sealed cell was stored in the dark, no change in electrochemical properties was observable even 4 weeks after preparation.

Sample Cell Holder and Electromagnet. A sample cell holder was constructed for control of the solution temperature (Figure 1). The holder was supported by the poles of the electromagnet such that the channel across the brass block enclosed the gap of the magnet. The voltammetric cell was held so that the working electrode was near the center of the gap. To ensure a fixed geometry in a set of experiments, the cell was not moved after its initial positioning.

The electromagnet was a compact device that was constructed locally. Its design has been detailed elsewhere.[8] It was energized by a regulated

---

(3) Liu, D. K. K.; Faulkner, L. R. *J. Am. Chem. Soc.* **1977**, *99*, 4594.

(4) Kim, J.; Ph.D. Thesis, University of Illinois at Urbana—Champaign, 1983.

(5) (a) Bezman, R.; Faulkner, L. R. *J. Am. Chem. Soc.* **1972**, *94*, 6317. (b) Michael, P. R.; Faulkner, L. R. *Ibid.* **1977**, *99*, 7754.

(6) House, H. O.; Peng, E.; Peet, N. P. *J. Org. Chem.* **1971**, *36*, 2371.

(7) Kim, J.; Faulkner, L. R. *Anal. Chem.* **1984**, *56*, 874.

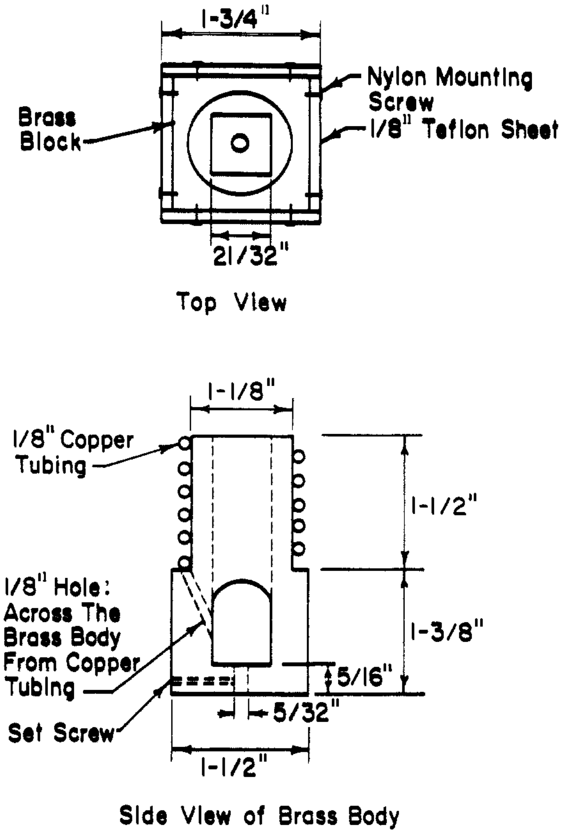

Figure 1. Insulated cell holder used to position the working electrode in the magnetic field and to maintain the temperature of the solution. The side view shows details of the brass body, while the top view shows the manner in which the body was clad in Teflon. The cell was held vertically in the square channel $^{21}/_{32}$ in. on a side. The light guide was mounted in the $^{5}/_{32}$-in. diameter hole at the bottom. The entire holder was mounted on the magnet by fitting the pole pieces into circular openings in the Teflon side plates. The magnetic axis would be perpendicular to the page. The flowing nitrogen was exhausted into the cell chamber through the diagonal hole in order to keep the cell free of frost.

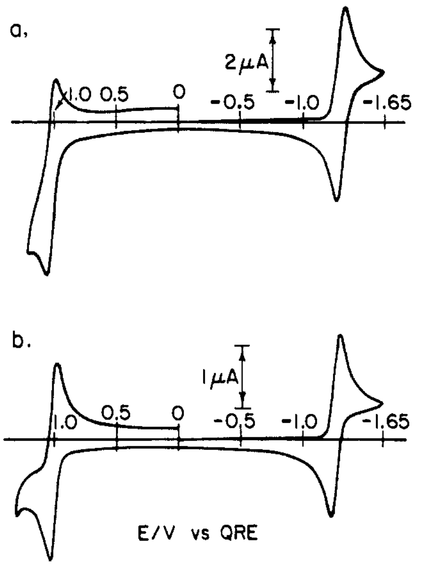

Figure 2. Cyclic voltammograms for 0.5 mM rubrene in DMF with 0.15 M $TBABF_4$ at (a) 22° and (b) −46 °C, scan rate = 100 mV/s. Scan begins at 0.0 V and first moves negatively. Cathodic currents are up.

Table I. Chronocoulometry for Rubrene[a] at −47 °C

		reduction[b] $R + e \rightleftharpoons R^{\bullet -}$	oxidation[c] $R + e \rightleftharpoons R^{\bullet -}$
Anson slope/μC $s^{-1/2}$	forward	2.15	2.52
	reverse	2.10	2.50
intercept/μC	forward	0.52	0.68
	reverse	0.54	0.61

[a] 0.5 mM rubrene in DMF with 0.15 M $TBABF_4$. [b] Initial potential = 0.0 V vs. QRE; step potential = −1.60 V; τ = 250 ms. [c] Initial potential = 0.0 V vs. QRE; step potential = +1.25 V; τ = 250 ms.

current supply also described elsewhere.[8] The magnetic field intensities were calibrated with a Model 615 gaussmeter (F. W. Bell).

Temperature Control. A flow of cold nitrogen gas was used to maintain the temperature of the cell. The apparatus was essentially the same as that described by Glass.[9,10] Temperature measurements were made with a thermistor (Fenwal Electronics GB31P22) located near the working electrode. At least 20 min was allowed for equilibration after a temperature change.

Experimental Procedures and Data Acquisition. A PARC Model 173 was used as the potentiostat throughout the work. For chronocoulometry, the working electrode was connected to a custom-built analogue charge follower. Cyclic voltammograms were recorded with an X-Y recorder.

A $^{1}/_{8}$-in. diameter fiber optic light guide (American Optical Corp.) was used to collect the ecl.[4,9,10] It was fixed below the working electrode by a set screw on the cell holder (Figure 1). The other end of the light guide was directed onto a Hamamatsu 928 photomultiplier contained in a magnetically shielded housing (Pacific Photometric Instruments Model 50B). The photocurrent was fed to a custom-built current-to-voltage converter.

The triple-step method[1] was used exclusively to generate ecl. Each experiment begins with the solution in a quiescent state and with the potential in a region where the solutes are not electroactive. The first step is made to a potential where one of the radical ions is generated at the diffusion-controlled rate. After a time t_f, the potential is changed to a value that allows the second radical ion to be generated, also at a diffusion-controlled rate. During this second step, an ecl transient appears as the two radical ions meet and react. Time measured into the second step from its leading edge is t_r. Normally, the second step lasts for a duration t_f; then the potential is returned to its initial value. Most of the remaining radical ions are then recollected at the electrode, and the light is extinguished.

The step potentials for ecl and chronocoulometry were set at values 200–250 mV past the cyclic voltammetric peaks, to ensure the immediate establishment of diffusion-controlled electrolysis. Uncompensated resistance in the voltammetric cell was not electronically compensated, because the electrode was filmed by the brief oscillations encountered when the positive feedback level was selected. The effect of noncompensation was negligible in the measurement of voltammetric parameters.

A minicomputer was used for potential control and for data acquisition in ecl and chronocoulometry. Details of the software and hardware have been described.[2k,4,5b,8-10]

In studies of magnetic field effects, ecl transients were obtained alternately at high field and at zero field. The two zero-field transients obtained before and after a high-field decay curve were averaged point-by-point, and this averaged zero-field transient was divided point-by-point into the high-field data to obtain intensity ratios. These ratios were then averaged over all data points to obtain mean enhancements for an entire transient. The results of magnetic field effect studies described below are averages of at least three such means. The details of this procedure have been described.[8]

The electrochemical behavior of the ecl systems was invariant in the presence of the magnetic field. This was also true for photocurrents generated by leaking light from a remote source into the detection system.

Results and Discussion

Electrochemical Behavior and Energetics. Figure 2 shows cyclic voltammograms of 0.5 mM rubrene in 0.15 M $TBABF_4$–DMF at 22 and −46°. The reversible formation of the rubrene radical anion produces peaks near −1.3 V. At all temperatures, the anion radical appeared stable. No difference in behavior is seen for this couple between the two temperature limits, except for the decreased peak heights due to the reduced diffusion rate at lower temperatures.

The voltammetry for the formation and rereduction of the rubrene cation radical is complicated at room temperature by background processes involving DMF. Most of the background interference is suppressed in cyclic voltammetry at −46 °C, but

---

(8) Morris, J. L., Jr. Ph.D. Thesis, University of Illinois at Urbana—Champaign, 1978.

(9) Glass, R. S.; Faulkner, L. R. *J. Phys. Chem.* **1981**, *85*, 1160.

(10) Glass, R. S.; Ph.D. Thesis, University of Illinois at Urbana—Champaign, 1980.

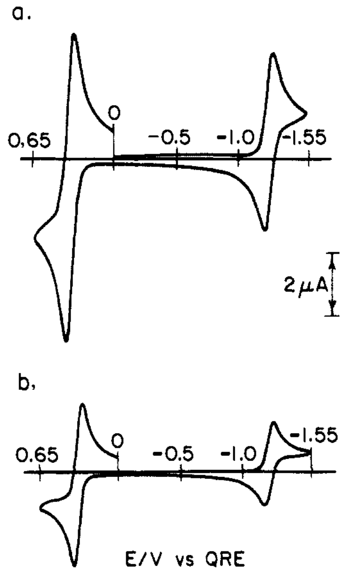

Figure 3. Cyclic voltammograms for 0.5 mM TMPD and 0.5 mM rubrene in DMF with 0.15 M $TBABF_4$ at (a) 21° and (b) -48 °C, scan rate = 100 mV/s. Scan begins at 0.0 V and first moves negatively. The peaks in the positive region are for TMPD.

Table II. Standard Free Energy of the Rubrene Ion Annihilation[a]

temp/C	$-\Delta G°$/eV
21	2.30
-21	2.29
-31	2.28
-47	2.28

[a] 0.5 mM rubrene in DMF with 0.15 M $TBABF_4$.

background effects were still observable by chronocoulometry at this temperature. For example, the forward and reverse Anson slopes[7,11] for oxidation of rubrene were 15% higher than those for reduction (Table I), whereas the cyclic voltammetric peak heights were similar for both processes. The *n* values estimated by our method of relating chronocoulometric and cyclic voltammetric data[7] were 0.88 for reduction ($R \rightarrow R^{\cdot-}$) and 0.64 for oxidation ($R \rightarrow R^{\cdot+}$). The background contributions to unusually high Anson slopes for oxidation are obvious.

The oxidation of TMPD produces very well-defined electrochemistry, even at room temperature. Figure 3 presents two cyclic voltammograms obtained at different temperatures for 0.1 M $TBABF_4$–DMF containing 0.5 mM TMPD and 0.5 mM rubrene. The peaks in the negative potential range are for rubrene, whereas the positive ones are for TMPD. The higher peak heights for TMPD indicate that the TMPD diffusion coefficient is greater than that of rubrene. The only differences between parts a and b in Figures 3 are smaller peak heights at the lower temperature, again due to the decreased diffusion rates. In chronocoulometry at room temperature, the forward Anson slope was 8.09 $\mu C/s^{1/2}$ and the reverse slope was 8.07 $\mu C/s^{1/2}$, giving a slope ratio of 0.998. The *n* measured by our method of transients was 0.96. This excellent behavior reflects two factors: (a) the DMF background contribution is small in the potential range of TMPD's electroactivity; and (b) hydrogen absorbed in platinum is neither oxidized nor reduced in that region.[7]

Table II lists the free energies, estimated from cyclic voltammograms, for the rubrene radical ion annihilation (reaction 3) at four different temperatures. There may be a decrease of $-\Delta G°$ as temperature drops, although the magnitude of the change is comparable to the precision of measurements. The standard free energy change for the ion annihilation between $TMPD^{\cdot+}$ and $R^{\cdot-}$ was -1.62 eV at room temperature. This energy was also not appreciably altered by temperature changes.

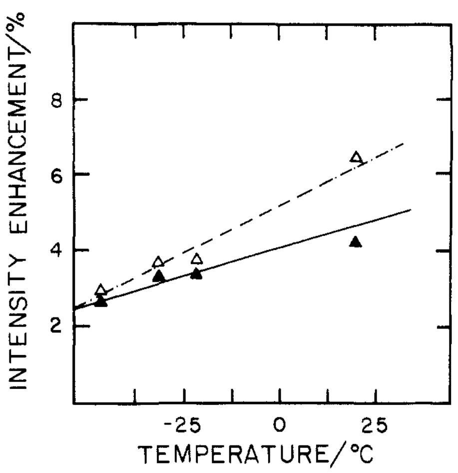

Figure 4. Magnetic field effect at 0.152 T (1.52 kG) for the rubrene system (solution was the same as for Figure 2): open triangles, anion generated first; filled triangles, cation generated first. t_f = 1 s.

Magnetic Field Effects. Figure 4 shows the temperature dependence of magnetic enhancements for ecl from 0.5 mM rubrene in 0.15 M $TBABF_4$–DMF. The field strength was held constant at 0.152 T. The field effect was different for the two reactant generation sequences, but in both cases the enhancement decreased monotonically with temperature. The enhancement remained observable even at -48 °C, where S-route kinetic behavior was dominant, both in the earlier work by Glass[2k] and in this study.

Magnetic enhancements of ecl are interpreted in terms of field effects on two types of reactions involving triplet intermediates, viz., the production of singlets via TTA (e.g., reaction 5) and the quenching of triplets by radical ions,[1,2g]

$$^3R^* + R^{\cdot+} \rightarrow R + R^{\cdot+} \qquad (8)$$

$$^3R^* + R^{\cdot-} \rightarrow R + R^{\cdot-} \qquad (9)$$

Fields of intermediate strength (0.1–0.5 T) have been shown to reduce the rate constants for both classes of reaction.[1] Arguments based on conservation of spin angular momentum have rationalized these observations successfully.[1,2g,12]

The field effect on ecl reflects counterbalancing tendencies. The inhibition of reaction 5 would reduce the ecl from the T route at high field, if other factors were not at work. Overriding this tendency is the inhibition of the quenching reactions, which are believed to control the triplet lifetime.[1,2g,13] The field effect on quenching increases the lifetime and allows the triplets to participate more efficiently in TTA. Since the ecl intensity depends normally on the square of the lifetime,[1,13] the net influence of the field is to enhance the ecl intensity.[1,2g,12,14]

The smaller enhancements at low temperature are consistent with a mixed S- and T-route mechanism having a T-route fraction that decreases with temperature. The fractional contributions of the two routes can be estimated by examining the temperature dependence of magnetic effects in a rubrene-based system that can produce ecl only via the T route. We have therefore studied the rubrene/TMPD system, wherein the rubrene triplet is the only energetically accessible excited product of electron transfer,[1,2g]

$$R^{\cdot-} + TMPD^{\cdot+} \longrightarrow {}^3R^* + TMPD \qquad (10)$$

$$\longrightarrow R + TMPD \qquad (11)$$

The results are depicted in Figure 5 for a field strength of 0.152 T. The solution was 0.1 M $TBABF_4$–DMF containing 0.5 mM

---

(11) (a) Anson, F. C. *Anal. Chem.* **1966**, *38*, 54. (b) Bard, A. J.; Faulkner, L. R. *Electrochemical Methods*; Wiley: New York, 1980.

(12) (a) Merrifield, R. E. *J. Chem. Phys.* **1968**, *48*, 4318. (b) Ern, V.; Merrifield, R. E. *Phys. Rev. Lett.* **1968**, *21*, 609. (c) Johnson, R. C.; Merrifield, R. E. *Phys. Rev. B* **1970**, *1*, 896. (d) Kearns, D. R.; Stone, A. J. *J. Chem. Phys.* **1971**, *55*, 3383. (e) Geacintov, N. E.; Swenberg, C. E. *Ibid.* **1972**, *57*, 378. (f) Atkins, P. W.; Evans, G. T. *Mol. Phys.* **1975**, *29*, 921.

(13) Morris, J. L., Jr.; Faulkner, L. R. *J. Electrochem. Soc.* **1978**, *125*, 1079.

(14) Faulkner, L. R.; Bard, A. J. *J. Am. Chem. Soc.* **1969**, *91*, 6495, 6497.

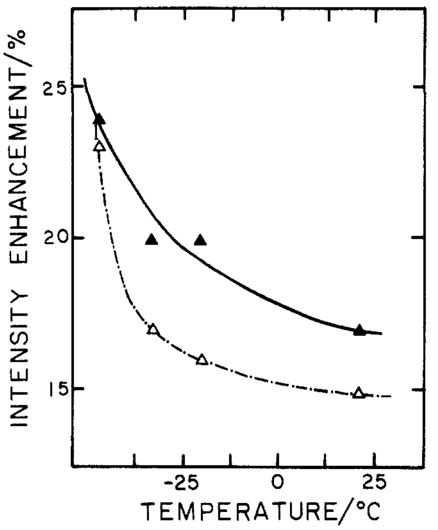

Figure 5. Magnetic field effect at 0.152 T (1.52 kG) for the rubrene-TMPD system (solution was the same as for Figure 3): open triangles, anion generated first; filled triangles, cation generated first. $t_f = 1$ s.

TMPD and 0.5 mM rubrene. In contrast with the rubrene system, there is a steep increase in the field effect as the temperature decreases. The differing behavior patterns can be usefully related via the following argument.

The intensity of ecl is proportional to the efficiency ϕ_{ecl} with which one redox event eventually yields a photon. In the rubrene system, there are two reaction pathways, so ϕ_{ecl} is the sum of efficiencies for the separate pathways and can be written,

$$\phi_{ecl} = \phi_f \phi_S{}^R + \phi_f \phi_T{}^R \phi_{TTA} \quad (12)$$

where ϕ_f is the fluorescence efficiency of $^1F^*$, $\phi_S{}^R$ is the fraction of electron-transfer events that produce excited singlets (via process 1), $\phi_T{}^R$ is the fraction of electron-transfer events that produce triplets (via process 2), and ϕ_{TTA} is the efficiency with which a triplet is converted to $^1R^*$ via TTA. The magnetic effect is normally understood as being confined to ϕ_{TTA}. Let us express the field dependence by writing ϕ_{TTA} as $\phi^0{}_{TTA} + \delta\phi_{TTA}$, where the first term is the zero-field triplet conversion efficiency and the second is the change is efficiency induced by the field. Now we can write the magnetic enhancement for the rubrene system at field H as,

$$E_R = [\phi_{ecl}(H) - \phi_{ecl}(0)]/\phi_{ecl}(0) \quad (13)$$

$$E_R = \phi_T{}^R\ \delta\phi_{TTA}/(\phi_S{}^R + \phi_T{}^R\ \phi^0{}_{TTA}) \quad (14)$$

For the rubrene/TMPD "mixed" system, the chemiluminescence efficiency is the efficiency of the T route,

$$\phi_{ecl} = \phi_f \phi_T{}^M \phi_{TTA} \quad (15)$$

where $\phi_T{}^M$ is the fraction of redox events that yield rubrene triplets via process 10. Again, the field effect ought to be wholly attributable to temperature dependence in the efficiency of converting $^3R^*$ to $^1R^*$ via TTA. Moreover, the kinetics of that conversion ought to be identical with those operating in the rubrene system, except for one step: reaction 8 is replaced by the analogous process,

$$^3R^* + TMPD^{\cdot+} \rightarrow R + TMPD^{\cdot+} \quad (16)$$

Within the framework of current understanding, this substitution is not expected to alter the magnetic effect on the triplet lifetime markedly, so we assume that the field effect on ecl from the rubrene/TMPD system is also characteristic of the effect on the T-route contribution to ecl from the rubrene system. Thus ϕ_{TTA} is taken as approximately the same for the two systems.

The magnetic enhancement for the mixed system, derived from definition 13, is

$$E_M = \delta\phi_{TTA}/\phi^0{}_{TTA} \quad (17)$$

Hence the ratio of the enhancement in the rubrene system to that in the mixed system at a common temperature is

$$\frac{E_R}{E_M} = \frac{\phi_T{}^R \phi^0{}_{TTA}}{\phi_S{}^R + \phi_T{}^R \phi^0{}_{TTA}} \quad (18)$$

This ratio is diagnostically valuable, for it is the fraction of ecl that arises in the rubrene system via the T route at zero field. The numerator is the efficiency with which the T route generates $^1R^*$, whereas the denominator is the sum of this efficiency and the efficiency of singlet production via the S route. From the data in Figures 4 and 5, one can therefore estimate that the fractional T-route contribution to rubrene ecl falls from 25–40% at room temperature to about 10% at -40 °C. These estimates are very much in accord with the observations of kinetic behavior made by Glass and Faulkner.[2k]

Our critical assumption is that $\delta\phi_{TTA}/\phi^0{}_{TTA}$ is a common function for all T-route ecl based on rubrene. In fact, it is known that magnetic enhancements vary with the pulse sequence and with the species, such as $TMPD^{\cdot+}$ or benzoquinone radical anion, that is paired with a rubrene radical ion to produce ecl from a mixed system.[1,2g] We consider our approximation as valid within perhaps a factor of 2, since this is about the range of enhancements seen in various mixed systems. The enhancement for the pure rubrene system is smaller than for mixed systems in all cases known to us; thus our argument is qualitatively consistent with other data.

The pulse sequence makes a difference in the intensity of ecl and in the magnetic enhancement. Since the ecl reaction zone is predicted to have essentially the same structure for both sequences,[13] these differences probably reflect electrolytic variations in the concentrations of trace impurities, such as oxygen, that can affect the triplet lifetime. We suggest from the arguments above that the T-route fraction is significantly higher for one pulse sequence than for the other at room temperature. We believe that it is entirely reasonable that this would be so.

We are not able to offer a detailed interpretation of the temperature dependence for the magnetic enhancement of ϕ_{TTA}. The rise in the enhancement at lower temperatures could simply imply that the triplet lifetime is more fully controlled by the radical ions than at room temperature. In fact, Kearns and Stone[12d] predicted that as viscosity increases the quenching of triplets by doublet species becomes relatively more effective in comparison with the encounter-limited rate. On the other hand, the dynamics of TTA might be altered by having slightly endothermic channels become less competitive in the colder media. Candidates include those to the first excited singlet (process 5) and to the second triplet.[3] In addition, there could be effects of temperature on the interchange of electron and nuclear spin angular momentum.[15] More experiments and better theory are needed to permit a confident interpretation of the observations in Figure 5.

Basis for the Mechanistic Change. Glass and Faulkner[2k] suggested two general rationales for the temperature dependence of ecl mechanism in the rubrene system.

First is the possibility that the efficiency of converting triplets to singlets via TTA (i.e., ϕ_{TTA}) becomes poorer at low temperatures. This could happen if the branching ratio for producing $^1R^*$ in TTA (reaction 5) falls off with temperature, perhaps because that channel is slightly endothermic. Another possibility is that the quenching of triplets by various species becomes more competitive relative to TTA at the lower temperatures.

The second general rationale is that the change in mechanism reflects a temperature dependence in the branching ratios for the primary electron-transfer event (i.e., $\phi_T{}^R$ and $\phi_S{}^R$). If the singlet channel (reaction 1) becomes relatively more favorable at lower temperature, the dominance of the S route in that regime would be readily understood. A change in the branching ratios might reflect alterations in the energy balances for reactions 1–3, or it

---

(15) (a) Schulten, K.; Staerk, H.; Weller, A.; Werner, H.-J.; Nickel, B. *Z. Phys. Chem. (Frankfurt/Main)* **1976**, *101*, 371. (b) Weller, A.; Staerk, H.; Treichel, R. *Faraday Discuss. Chem. Soc.* **1984**, *78*, 271–278. (c) Staerk, H.; Kühnle, W.; Treichel, R.; Weller, A. *Chem. Phys. Lett.* **1985**, *118*, 19.

might arise from an alteration in the reaction environment.

One cannot favor either rationale on the basis of the kinetic studies and the magnetic effects, but it is possible to draw conclusions by examining the effects of temperature on ϕ_{ecl}.

Temperature Dependence of Ecl Efficiency. For any ecl system, the relationship between the absolute light intensity I (einsteins/s) and the total rate of electron transfer N (mol/s) is

$$I = \phi_{ecl} N \tag{19}$$

For the rubrene system, both the oxidant and the reductant are generated from the same precursor. In such a case, the analytical solution for the reaction rate during the second step of the triple-step sequence is[16]

$$N = AD^{1/2}C_P{}^{*}t_f{}^{-1/2}[0.896(t_r/t_f)^{-1/2} - 0.865] \tag{20}$$

where A is the electrode area, D is the diffusion coefficient of the precursor, and $C_P{}^{*}$ is the bulk concentration of the precursor.

The observed light transient I_{obsd} is normally an uncalibrated signal proportional to I. The constant of proportionality G includes geometric and sensitivity factors. If ϕ_{ecl} is approximately constant during the experiment, the relative intensity will take a form that is linear in $(t_r/t_f)^{-1/2}$

$$I_{obsd} = a_{obsd}(t_r/t_f)^{-1/2} - b_{obsd} \tag{21}$$

where $a_{obsd} = G\phi_{ecl}0.896AD^{1/2}C_P{}^{*}t_f{}^{-1/2}$.

By taking the ratio of the slope of the linearized ecl transient a_{obsd} and the Anson slope from chronocoulometry (i.e., $2nFAD^{1/2}C_P{}^{*}\pi^{-1/2}$),[11] one obtains

$$\frac{a_{obsd}}{\text{Anson slope}} = \phi_{ecl}\frac{0.896\pi^{1/2}G}{2nFt_f{}^{1/2}} \tag{22}$$

Except for ϕ_{ecl}, all factors in this ratio are constant with a fixed experimental setup and for a particular t_f. Thus relative changes in ϕ_{ecl} can be measured over a temperature range by recording ecl and chronocoulometric transients at each of several temperatures and taking the ratio of slopes at each temperature. The precision and accuracy of the method can be on the order of a few percent.

The chief requirement for applying the method is that the light transient be linearizable in the form indicated by eq 21. Thus ϕ_{ecl} must be nearly independent of time. If the rubrene system were purely an S-route case, this could be assumed reliably, because ϕ_{ecl} would equal $\phi_S{}^R\phi_f$, and neither factor could be appreciably time dependent.[9] The efficiency $\phi_S{}^R$ is a branching ratio for an elementary process, and the singlet lifetime is too short for time-dependent quenching to influence ϕ_f. In general, the T route introduces a time dependence to ϕ_{ecl}, because ϕ_T is influenced by bimolecular processes.[13,17] Even so, ϕ_{ecl} may remain sufficiently constant to produce reasonably linearizable light transients,[17] so that one can study changes in relative ϕ_{ecl} with satisfactory confidence.

Even at room temperature, the light transients from the rubrene system showed good linearity vs. $(t_r/t_f)^{-1/2}$ (correlation coefficient >0.987) when the anion was generated first (Figure 6). The correlation coefficient increased systematically as the temperature was lowered. The slope ratios indicated in eq 22 were determined at different temperatures and were normalized by the highest value to get relative chemiluminescence efficiencies. The results are depicted in Figure 7 for several concentrations of the supporting electrolyte.

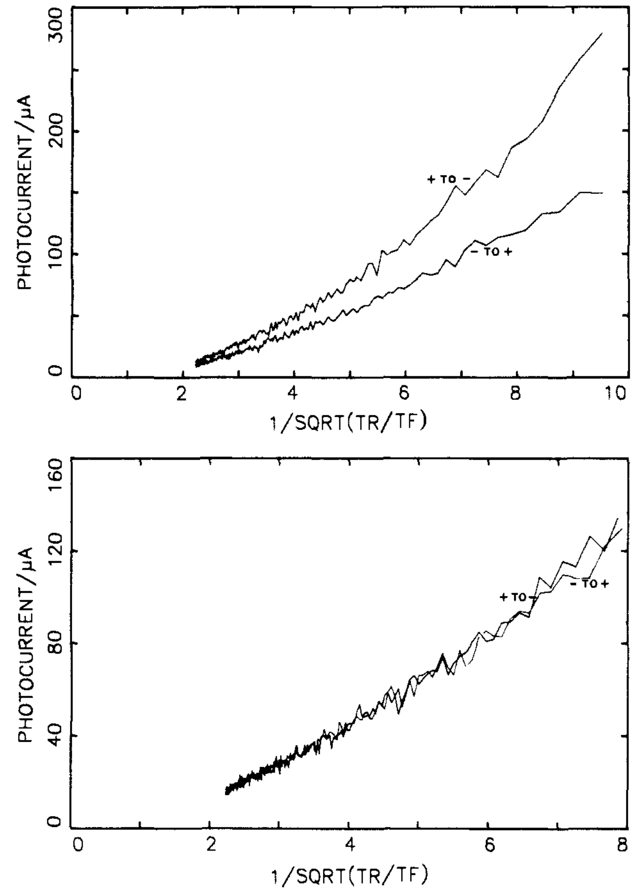

Figure 6. Chemiluminescence intensity vs. the time parameter for the rubrene system at 21° (top) and –46 °C (bottom). Solution was the same as for Figure 2. t_f = 1 s.

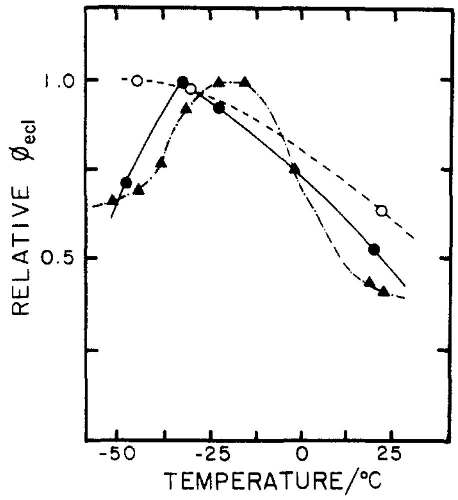

Figure 7. Temperature dependence of relative chemiluminescence efficiency for rubrene systems with different supporting electrolyte concentrations. Open circles, filled circles, and triangles are for 0.1, 0.15, and 0.2 M TBABF$_4$, respectively.

A most important feature of the data in Figure 7 is that ϕ_{ecl} increases as the temperature is lowered from room temperature, regardless of the supporting electrolyte concentration. This result can be related to the factors in eq 12. A trivial explanation is that ϕ_f rises at lower temperatures, but since the fluorescence efficiency of rubrene is nearly unity at room temperature,[18] this cause can be ruled out. It must therefore be true that either the S route or the T route becomes more efficient at lower temperatures. On the other hand, we have found that the fractional T route contribution declines toward lower temperatures, so the gain in efficiency cannot be confined to the T route. One must conclude that the S route becomes more efficient at lower temperatures as a consequence of a rise in $\phi_S{}^R$. In other words, the branching ratios for the primary electron-transfer event must be altered by

---

(16) Faulkner, L. R. *J. Electrochem. Soc.* **1977**, *124*, 1724.

(17) (a) Feldberg, S. W. *J. Phys. Chem.* **1966**, *70*, 3928. (b) Bezman, R.; Faulkner, L. R. *J. Am. Chem. Soc.* **1972**, *94*, 3699.

(18) Stevens, B.; Algar, R. E. *J. Phys. Chem.* **1968**, *72*, 2582.

the temperature. The results in Figure 7 for 0.15 M supporting electrolyte imply that $\phi_S{}^R + \phi_T{}^R\phi_{TTA}$ doubles in going from room temperature to about −31 °C, while the magnetic data suggest that the ratio in eq 18 drops from about 0.4 to 0.2 over the same range. Therefore, $\phi_S{}^R$ seems to rise by about 170%, while $\phi_T{}^R\phi_{TTA}$ falls by about 60%. We cannot say what happens individually to $\phi_T{}^R$ and ϕ_{TTA}.

In seeking an explanation for the change in the product distribution of electron transfer, one is naturally drawn to the energetics of channels 1–3. Since the values in Table II indicate that the free energy available from the redox reaction changes by no more than about kT over the entire temperature range, a rationale based entirely on energetics must focus on differences in activation energies for the three channels, rather than on changes in the accessibility of products. Even if the rate constants for all of the channels fell with temperature, the yield $\phi_S{}^R$ would rise if the rate constants for channels 2 or 3 fell more sharply than that for channel 1. Thus the activation energy for channel 1 would have to be substantially smaller than that for one of the remaining channels. It is conceivable that this is so, but we are not in a position to project details, because of the theoretical uncertainty surrounding channels 2 and 3. These are both in the "inverted" region, in the terminology of the Marcus theory, and both may be influenced by nuclear tunneling.[1,19] In fact, Marcus theory predicts that both channels will be practically inoperative.[1,19] An interesting possibility is that the triplets arise not by direct population in the manner suggested in eq 2, but instead via the second triplet[19c] ${}^3R_2{}^*$,

$$R^{\cdot+} + R^{\cdot-} \rightarrow {}^3R_2{}^* + R \rightarrow {}^3R^* + R \qquad (23)$$

If the first excited singlet lies slightly below the second triplet, the activation energy for production of triplets would exceed that for production of singlets, and our results would be rationalized. Still, one should not get too deeply into this kind of argument, because other features of the data in Figure 7 indicate that the reaction energetics do not tell the whole story.

Effects of Electrolytes. In Figure 7, one can see that the concentration of the $TBABF_4$ has a marked effect on the temperature dependence of ϕ_{ecl}. When the electrolyte concentration was 0.1 M, the relative ϕ_{ecl} increased monotonically as temperature decreased, but at higher concentrations ϕ_{ecl} passed through a maximum. At 0.15 M, the maximum efficiency was observed at −31 °C, but at 0.2 M it was found at −21 °C. There is no temperature range over which the curves in Figure 7 are isomorphic; hence the supporting electrolyte must be a yield-controlling species with respect to the primary redox process under all studied conditions. This is a quite unexpected result.

The most obvious effect of supporting electrolytes in ecl is the formation of ion pairs or higher aggregates involving the radical ions. Since the solvents usually employed have fairly high dielectric constants (37 for DMF), supporting electrolytes have been generally regarded as inert. Their influence on ecl has been investigated only in THF, a medium of low dielectric constant.

Keszthelyi et al.[20] studied the 9,10-dimethylanthracene (DMA)/tri-*p*-tolylamine (TPTA) system in THF and observed that the ecl efficiency decreased as the concentration of tetra-*n*-butylammonium perchlorate was increased. They ascribed their results to a decrease in redox enthalpy ($-\Delta H°$) caused by a stabilization of the radical ions by ion pairing. In support of this view, they found higher magnetic field effects in solutions containing higher concentrations of supporting electrolytes, a trend that was taken as evidence that the T route became relatively more important as the redox enthalpy decreased. This system involves exciplex intermediates,[1,21] which have since been shown to be dynamically and statically quenched by supporting electrolytes,[22] so it is difficult now to be sure of the interpretation.

The effects reported here are almost certainly not the result of alterations of the energetics by ion pairing. Consider only the data in Table II, which show that the free energy of reaction does not change significantly, even at the lowest temperature, which is below the maximum in ϕ_{ecl}. In general, standard potentials for couples involving radical ions in DMF do not shift with changes in the concentration of electrolytes composed of large, spherical ions,[23] so pairing of the radical ions does not involve appreciable binding energies, and only loose aggregations probably could be considered to exist here. To explain our observations, one must consider influences aside from energetics. These could include an influence on the mechanisms for conservation of angular momentum[15] or an alteration in the reaction coordinate induced by collisions between an ion of the electrolyte and a pair of ions in an encounter complex. Another possible effect of the electrolyte population is to introduce a screening effect that increases the mean distance between radical ions at the moment of electron transfer. A fourth prospect is that the electrolyte alters the vibrational mode distribution in the reaction environment. Additional experiments will be needed to define the matter further.

The sharp breakoff of relative ϕ_{ecl} at very low temperatures in solutions of higher supporting electrolyte concentrations is a striking effect and suggests that a transition takes place in the structure of the reaction complex. We are not now able to comment further on this feature.

Conclusions

Light production in the rubrene system now seems well established as arising from a mixture of S and T routes with a decreasing T-route fraction as the temperature decreases. The decline of the T-route fraction occurs mainly because there is a rise in the yield of ${}^1R^*$ produced directly by electron transfer. Since the T route generates a measurable fraction of the light at all temperatures, it is probably true that the yield of ${}^3R^*$ in electron transfer is rather high, perhaps several tens of percent. Given the poor efficiency of converting triplets to emitting singlets,[1,13,24] one could not explain the competitiveness of the T route if the triplet production efficiency in electron transfer were as low as a few percent. The concentration of the supporting electrolyte markedly affects the distribution of products from the primary redox process. All of these points can be drawn from the qualitative features of our data and the earlier results of Glass,[2k] and they seem rather secure.

Above, we made numeric estimates of the S- and T- route fractions at different temperatures, and we projected percentage changes vs. temperature of S- and T-route efficiencies. The validity of these numbers rests upon the assumption that $\delta\phi_{TTA}/\phi_{TTA}$ has the same behavior with field strength in both the rubrene system and the rubrene/TMPD system. The assumption and the numbers all seem appropriate (at least roughly), but the assumption deserves direct experimental test via studies of delayed fluorescence.

Two new techniques were developed in this work. The method of relating magnetic enhancements between systems may be generally applicable as a means for quantifying the fractional contribution of the T route. It requires further validation. On

---

(19) (a) Marcus, R. A. *Annu. Rev. Phys. Chem.* **1964**, *15*, 155. (b) Marcus, R. A. *J. Chem. Phys.* **1965**, *43*, 2654; **1970**, *52*, 2803. (c) VanDuyne, R. P.; Fischer, S. F. *Chem. Phys.* **1974**, *5*, 183. (d) Siders, P.; Marcus, R. A. *J. Am. Chem. Soc.* **1981**, *103*, 741, 748. (e) Newton, M. D.; Sutin, N. *Annu. Rev. Phys. Chem.* **1984**, *35*, 437–480. (f) Liu, D. K.; Brunschwig, B. S.; Creutz, C.; Sutin, N. *J. Am. Chem. Soc.* **1986**, *108*, 1749.

(20) Keszthelyi, C. P.; Tokel-Takvoryan, N. E.; Tachikawa, H.; Bard, A. J. *Chem. Phys. Lett.* **1973**, *23*, 219.

(21) (a) Weller, A.; Zachariasse, K. *Chem. Phys. Lett.* **1971**, *10*, 5. (b) Weller, A. In *The Exciplex*; Gordon, M., Ware, W. R., DeMayo, P., Arnold, D. R., Eds.; Academic Press: New York, 1975; p 23. (c) Zachariasse, K. A. *Ibid.*, p 275.

(22) (a) Simon, J. D.; Peter, K. S. *J. Am. Chem. Soc.* **1981**, *103*, 6403. (b) Simon, J. D.; Peters, K. S. *Ibid.* **1982**, *104*, 6142. (c) Simon, J. D.; Peters, K. S. *Ibid.* **1983**, *105*, 4875. (d) Kitamura, N.; Imabayashi, S.; Tazuke, S. *Chem. Lett.* **1983**, 455. (e) McCullough, J. J.; Yeroushalmi, S. *J. Chem. Soc., Chem. Commun.* **1983**, 254. (f) Goodson, B. E.; Schuster, G. B. *J. Am. Chem. Soc.* **1984**, *106*, 7254. (g) Hartley, R. J.; Faulkner, L. R. *Ibid.* **1985**, *107*, 3436.

(23) Peover, M. E. *Electroanal. Chem.* **1967**, *2*, 1.

(24) (a) Parker, C. A.; *Photoluminescence of Solutions*; Elsevier: Amsterdam, 1968. (b) Liu, D. K. K.; Faulkner, L. R. *J. Am. Chem. Soc.* **1978**, *100*, 2635.

the other hand, the evaluation of relative chemiluminescence efficiencies via the correlation of linearized light transients and chronocoulometric data seems firmly based, attractively precise, and applicable to a wide range of systems. It deserves further use.

Particularly intriguing in this work were the effects of the electrolytes on ecl dynamics. Concentrated study of them offers genuine promise for illuminating the elements that control chemiexcitation pathways in condensed phases. New work should be undertaken in that direction.

Acknowledgment. We are grateful to the National Science Foundation for supporting this work under Grants CHE-81-06026 and CHE-86-07984.

Contrasting One- and Two-Cation Binding Behavior in *syn*- and *anti*-Anthraquinone Bibracchial Podand (BiP) Mono- and Dianions Assessed by Cyclic Voltammetry and Electron Paramagnetic Resonance Spectroscopy

Milagros Delgado, Deborah A. Gustowski, Hyunsook K. Yoo, Vincent J. Gatto, George W. Gokel,* and Luis Echegoyen*

Contribution from the Department of Chemistry, University of Miami, Coral Gables, Florida 33124. *Received June 19, 1987*

Abstract: Two new, bibracchial (two-armed) podands (BiPs) based on the anthraquinone ring systems have been prepared. Each has $CH_3O(CH_2CH_2O)_3$ side arms attached in the 1,5 (*anti*-BiP) and 1,8 positions (*syn*-BiP). Reduction of these species either electrochemically or using a reducing metal affords mono- and/or dianions which show significantly different cation affinities depending upon whether or not the side arms are positioned in such a way that cooperation in cation binding may occur. Electron paramagnetic resonance (EPR) results clearly show that reduced *anti*-BIP sequentially binds two cations, obviously from opposite sides, and does so with considerable strength. Remarkably, reduced *syn*-BiP binds two sodium cations as well, apparently on the same side of the anthraquinone residue. Evidence for the latter observation is found in two Na^+ coupling constants of 0.7 G and an increase in total spectral width by nearly a factor of 2. The lithium binding enhancement observed by cyclic voltammetry (0.46 V) with *anti*-BiP is the largest cation binding enhancement yet reported for any switchable lariat ether or podand. Results are compared with a 1,8-anthraquinone-derived crown ether having a total of six oxygen donors in the macroring. Evidence is presented that this crown is an exceptionally strong cation binder not only when reduced (Na^+ coupling constant = 1.43 G), but in its neutral form as well.

The anthraquinone system is an especially interesting one for the study of reducible and switchable lariat ethers[1] because its anion is stable for months in water so long as oxygen is excluded.[2] Although podands (noncyclic polyethylene glycols) generally exhibit poor cation binding,[3] when combined with the semiquinone nucleus, very strong cation complexation is observed for the radical anion.[4] We have recently demonstrated that anthraquinone podands can be used for electrochemically switched cation transport in bulk organic membranes[1d] and have further demonstrated that both monoanion and dianion species can be formed and detected.[1a] In previous work, we have shown that both one- and two-electron reduction can lead to enhanced cation binding in anthraquinone-derived podands and lariat ethers.[1b,c] We have referred to the ability of these systems to exhibit differing cation affinities depending upon whether the radical ion or the dianion is formed as tunability.[1b,c]

We report here our efforts to expand the concept of tunability to include not only the formation of anion and dianion, but the cooperation of these reducible species with one or more side arms adjacent to each other, on opposites sides of the reducible nucleus, and in a macroring. We thus explore the potential for four entries to tunability, namely, one- and two-electron reduction coupled with side-arm and macroring placement. The bulk of the evidence presented here derived from electron paramagnetic resonance studies, so the principal focus of this work is one and/or two cations interacting with the radical anion of anthraquinone (one-electron reduction).

Results and Discussion

Ligand Syntheses. Three substituted anthraquinone derivatives were prepared for the studies reported here. They are shown in Scheme I as **1** (*syn*-BiP), **2** (*anti*-BiP), and **3**. Compounds **1** and **3** were prepared from 1,8-dichloroanthraquinone, and **2** derives from 1,5-dichloroanthraquinone. The podands were prepared by treatment of 1,5- or 1,8-dichloroanthraquinone with the anion (NaH, THF) of $CH_3(OCH_2CH_2)_3OH$. The crown was prepared similarly except that the dianion of tetraethylene glycol was utilized. Details of the procedure for this nucleophilic aromatic substitution reaction are recorded in the Experimental Section.

Dimer crowns, i.e., bis(anthraquinone) crowns, have been previously reported by Akiyama and co-workers.[5] These compounds were prepared by the reaction of 1,8-dihydroxyanthraquinone with mono-, di-, or triethylene glycol ditosylate. This more traditional approach, according to the report,[5] yielded no crowns of the type disclosed here.

---

[1] (a) Echegoyen, L.; Gustowski, D. A.; Gatto, V. J.; Gokel, G. W. *J. Chem. Soc., Chem. Commun.* **1986**, 220. (b) Gustowski, D. A.; Delgado, M.; Gatto, V. J.; Echegoyen, L.; Gokel, G. W.; *Tetrahedron Lett.* **1986**, 3487 (c) Gustowski, D. A.; Delgado, M.; Gatto, V. J.; Echegoyen, L.; Gokel, G. W.; *J. Am. Chem. Soc.* **1986**, *108*, 7553. (d) Echeverria, L.; Delgado, M.; Gatto, V. J.; Gokel, G. W.; Echegoyen, L.; *Ibid.* **1986**, *108*, 6825.

[2] (a) Stone, E. W.; Maki, A. H. *J. Chem. Phys.* **1962**, *36*, 1944. (b) Stauff, J. *Photochem. Photobiol.* **1965**, *4*, 1199.

[3] (a) Voegtle, F.; Weber, E. *Angew. Chem., Int. Ed. Engl.* **1979**, *18*, 753. (b) Chan, L. L.; Smid, J. *J. Am. Chem. Soc.* **1967**, *89*, 4547. (c) Chan, L. L.; Wong, K. H.; Smid, J. *Ibid.* **1970**, *92*, 1955. (d) Helgeson, R. C.; Weisman, G. R.; Toner, J. L.; Tarnowski, T. L.; Chao, Y.; Mayer, J. M.; Cram, D. J. *Ibid.* **1979**, *101*, 4929.

[4] (a) Bock, H.; Hierholzer, B.; Voegtle, F.; Hollman, G. *Angew. Chem. Int. Ed. Engl.* **1984**, *23*, 57. (b) Wolf, R. E.; Copper, S. R.; *J. Am. Chem. Soc.* **1984**, *106*, 4646. (c) Maruyama, K.; Sohmida, H.; Tsukube, H. *Tetrahedron Lett.* **1985**, *26*, 3583.

[5] Nakatsuji, S.; Ohmori, Y.; Iyoda, M.; Nakashima, K.; Akiyama, S. *Bull. Chem. Soc. Jpn.* **1983**, *56*, 3185.

0002-7863/88/1510-0119$01.50/0